RESEARCH PAPER

Neuroprotective effect of Intranasal Co-Delivery of Chrysin and Daidzein PLGA Nanocarriers in Rotenone-Induced Parkinsonian disease in Experimental animals

Neelam L. Dashputre*[1], Umesh D. Laddha*[2], Vishal D. Dhopare [1], Smita P. Kakad[2], Anjali B. Tajanpure[1], Shubham J. Khairnar[1], Deepak S. Bhambere[2], Sunita N. Surse[3], Mansi V. Yeole[1]

[1]Department of Pharmacology, MET's Institute of Pharmacy, Bhujbal Knowledge City, Adgaon, Nashik-422003. Affiliated to Savitribai Phule Pune University, Pune, Maharashtra, India.

[2]Department of Pharmaceutics, MET's Institute of Pharmacy, Bhujbal Knowledge City, Adgaon, Nashik-422003. Affiliated to Savitribai Phule Pune University, Pune, Maharashtra, India.

[3]Department of Pharmacognosy, MET's Institute of Pharmacy, Bhujbal Knowledge City, Adgaon, Nashik-422003. Affiliated to Savitribai Phule Pune University, Pune, Maharashtra, India.

***Details of Corresponding Author:**

Dr. Neelam L. Dashputre

Associate Professor, Department of Pharmacology, METs,
Institute of Pharmacy, Bhujbal Knowledge City, Adgaon,
Nashik-422003, Maharashtra, India.

Email: neelamd_iop@bkc.met.edu

2. Dr. Umesh D. Laddha

Assistant Professor, Department of Pharmaceutics, METs, Institute of Pharmacy, Bhujbal Knowledge City, Adgaon, Nashik-422003, Maharashtra, India.

Email: umeshl_iop@bkc.met.edu

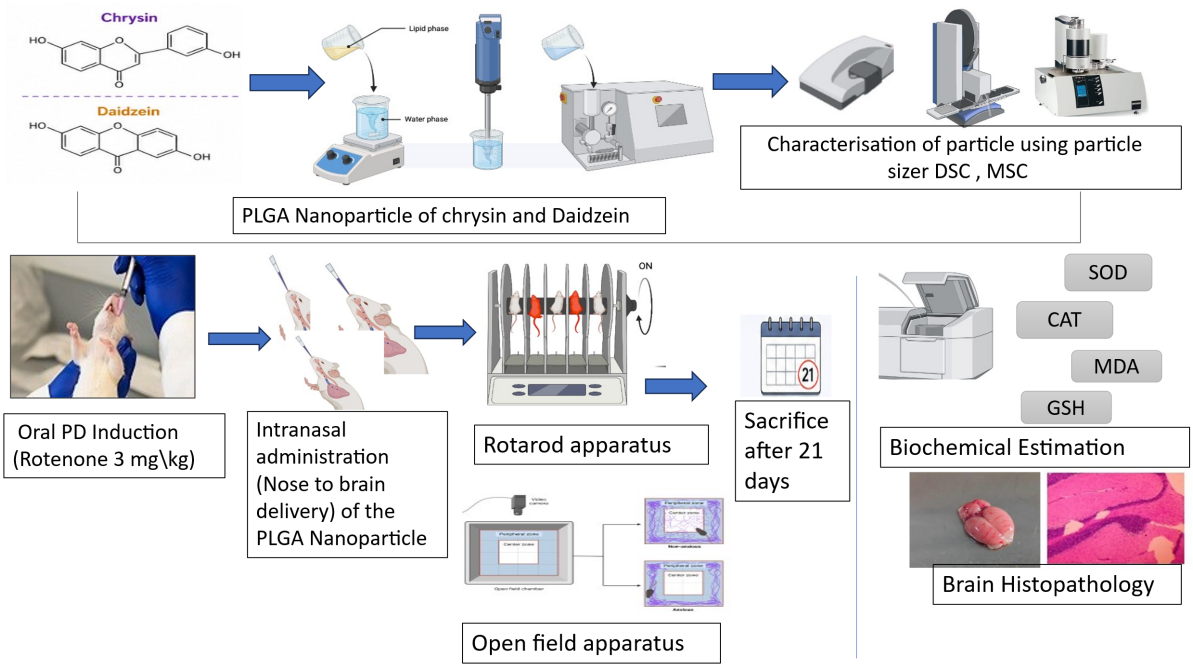
ABSTRACT:

Parkinson's disease (PD) is managed largely through symptomatic therapies, yet delivering therapeutic agents to the brain effectively and safely remains a major challenge. Nanotechnology offers strategies for improving drug disposition and potentially modifying disease progression. Chrysin and daidzein are flavonoids of interest for their possible neuroprotective effects, but their usefulness after oral administration is constrained by poor solubility and extensive presystemic metabolism. In this study, chrysin- and daidzein-loaded nanoparticles were developed for intranasal administration to improve bioavailability and brain delivery. The formulation was prepared by solvent evaporation and assessed for physicochemical characteristics and activity in a rotenone-induced rat model. The reported particle sizes were 196.1 and 170 nm, entrapment efficiencies were 94% and 93%, and zeta potentials were −20 and −23.8 mV for chrysin and daidzein, respectively. At 24 h, the reported in vitro and ex vivo release values were 90.52% and 68.7%. The formulation did not produce nasal mucosal irritation. Animals receiving the chrysin–daidzein combination showed higher dopamine levels than the comparison groups. Improvements in SOD, GSH, and catalase also indicated a potential antioxidant effect.

In vivo findings were consistent with improved brain targeting following intranasal delivery of chrysin and daidzein. The treated animals showed reduced parkinsonian symptoms, higher dopamine levels, improved oxidative-stress markers, and greater brain levels of chrysin. These observations suggest that intranasal administration of the phytoconstituents may help address the poor oral bioavailability that limits their use as a potential brain-directed intervention for Parkinson's disease.

Key words: PLGA Nanoparticles, Nose-to-brain delivery, Nanotechnology, polymeric drug delivery systems, Parkinson's disease.

Graphical Abstract:



How to cite this article: Neelam L. Dashputre*1 Umesh D. Laddha*2 Vishal D. Dhopare 1 Smita P. Kakad2 Anjali B. Tajanpure1 Shubham J. Khairnar1 Deepak S. Bhambere2 Sunita N. Surse3 Mansi V. Yeole1. Neuroprotective effect of Intranasal Co-Delivery of Chrysin and Daidzein PLGA Nanocarriers in Rotenone-Induced Parkinsonian disease in Experimental animals. Int J Drug Deliv Technol. 2026;16(90s):1131-1142. DOI: 10.25258/ijddt.16.90s.111.

1. INTRODUCTION:

Parkinson's disease (PD) is a progressive neurodegenerative disorder associated with the loss of dopamine-producing neurons in the substantia nigra. It produces both motor and non-motor symptoms and is the second most common neurodegenerative disease after Alzheimer's disease. As populations age, the burden of PD is expected to increase, reinforcing the need for improved therapeutic approaches. Estimates indicate that PD affects approximately 1–2% of people older than 60 years and as many as 3.5% of those aged 85–89 years. Symptoms commonly begin between 55 and 65 years of age. The disorder affects about 0.3% of the general population and is reported more frequently in men than women, although estimates of variation across ethnic and geographic groups remain inconsistent.

A central feature of PD is reduced dopamine in the striatum following degeneration of dopaminergic neurons in the substantia nigra pars compacta. The resulting disruption of basal-ganglia circuits contributes to impaired movement. Mechanisms associated with the disease include oxidative stress, mitochondrial impairment, neuroinflammation, α-synuclein aggregation, and apoptosis. Most cases are considered idiopathic, with age, oxidative stress, genetic variants such as SNCA, LRRK2, and PARK2, environmental exposures including pesticides and heavy metals, and altered protein function among the factors implicated in disease development.

Available medicines including levodopa, dopamine agonists, monoamine oxidase-B inhibitors, catechol-O-methyltransferase inhibitors, amantadine, and anticholinergics—primarily help control symptoms. Their clinical utility may nevertheless be limited by adverse effects, first-pass metabolism, low bioavailability, and restricted penetration across the blood–brain barrier. Nanocarriers, including liposomes, micelles, nanofibres, and nanoemulsions, are being explored to improve drug solubility, stability, pharmacokinetics, and delivery to the brain. Chrysin (5,7-dihydroxyflavone), a plant- and honey-associated bioflavonoid, has been investigated for antioxidant activity involving NRF2 activation and anti-inflammatory effects associated with NF-κB inhibition. Its lipophilicity and extensive metabolism, however, contribute to very low reported oral bioavailability (<0.02%). Intranasal administration may provide access to the central nervous system through olfactory and trigeminal pathways without an invasive procedure, although absorption can be limited by the available mucosal area and the drug's solubility [1].

Nanoemulsions are optically isotropic mixtures of water, oil, surfactant, and often a co-surfactant. By improving drug solubilization and mucosal permeation, these systems have been investigated as carriers for nasal delivery. In rotenone-induced rat models, formulations containing chrysin and daidzein have been assessed using physicochemical tests, in vitro diffusion studies, and behavioural measures such as locomotor activity and catalepsy. The limited availability of disease-modifying treatments for PD makes neuroprotective compounds and delivery approaches of interest.

Intranasal systems may improve brain exposure and could potentially reduce systemic adverse effects, although these possibilities require careful experimental validation.

PD is an age-associated neurological disorder characterized by symptoms that can include resting tremor, rigidity, bradykinesia, and postural instability. Onset often occurs between 55 and 65 years of age. Epidemiological estimates suggest that approximately 1–2% of people older than 60 years and 3.5% of those aged 85–89 years are affected; prevalence is also reported to be higher in men. Evidence concerning differences between ethnic groups is mixed. In some individuals, symptoms develop gradually, with a mild tremor in one hand among the early signs.

In addition to tremor, people with PD may experience stiffness, slowed movement, reduced facial expression, diminished arm swing while walking, and changes in speech. Symptoms generally progress over time. Population ageing is expected to increase the number of people living with PD; one cited projection anticipated an increase of more than 30% in incidence and prevalence by 2030. Common oral treatments, including levodopa and dopamine agonists, are used to manage symptoms, but they do not remove the challenges associated with effective drug delivery [1].

The intranasal route has attracted interest for central nervous system delivery because it is non-invasive and can exploit olfactory and trigeminal nerve pathways. Several carrier approaches have been investigated for chrysin delivery. Prior work has reported effects of intranasally delivered chrysin and daidzein on rotenone-associated cognitive changes in rats. However, the limited surface area of the nasal epithelium and the poor aqueous solubility of these compounds may constrain absorption. Nanoemulsions have therefore been explored as a way to address solubility and permeability limitations.

These systems generally contain water, oil, a surfactant, and a co-surfactant that helps solubilize the drug. Their thermodynamic stability and optical clarity make them useful candidates for formulation development. Published studies have reported improved pharmacokinetic properties for some nanoemulsion-based medicines delivered through nose-to-brain pathways.

The present work developed a nasal nanoformulation of chrysin and daidzein with the aim of improving solubility, brain targeting, and therapeutic performance. The formulations were characterized physicochemically and evaluated for in vitro diffusion and in vivo effects in disease-model rats. Behavioural outcomes, including locomotor activity and catalepsy, were assessed, while brain distribution of chrysin and biochemical measures—including dopamine and glutathione—were examined to investigate the response to intranasal treatment.

Whether PLGA-based nanoparticles carrying both chrysin and daidzein can reduce rotenone-induced behavioural and neurochemical changes remains insufficiently established. Accordingly, this study examined the potential neuroprotective effects of intranasally administered chrysin- and daidzein-loaded PLGA nanoparticles in a rat model of Parkinsonism.

2. Material and method:

2.1 Experimental animals

Male Wistar rats weighing 200–250 g were obtained from LACSMI Bio Farms (Laboratory Animal Centre for Cafe Medical Innovations), 12 “Rachana Blossom,” Jagdishnagar, Aundh, Pune, India. Animals had free access to food and water and were housed in polyacrylic cages under standard conditions: 22 ± 2 °C, 55–60% relative humidity, and a 12-h light/dark cycle beginning at 7:00 a.m. Behavioural testing was performed between 19:00 and 23:00 h, corresponding to the animals’ active phase. The protocol was approved by the Institutional Animal Ethics Committee under approval 1344/PO/Re/S/10/CCSEA; protocol MET-IOP-IAEC/2023-24/04 was conducted in accordance with CCSEA guidance for the care and use of experimental animals.

2.2 Drugs and chemicals

Chrysin was obtained from Yucca Enterprises Pvt. Ltd. (Mumbai, India), and daidzein from Otto Chemicals Pvt. Ltd. Rotenone was sourced from TCI Chemicals Pvt. Ltd. PLGA 50:50 (RESOMER®) was supplied by Evonik Pvt. Ltd. (Mumbai, India). Acetone, polysorbate 80, potassium dihydrogen orthophosphate, and dipotassium hydrogen phosphate were purchased from SDFCL, Mumbai. Polyvinyl alcohol was obtained from Thomas Baker, Mumbai, India. Other reagents and solvents were of analytical grade. Drug and reagent solutions were freshly prepared before use.

2.3 Experimental procedure

The animals were allocated randomly to six groups, with six rats per group. Group I served as the normal control and received sunflower oil (1 mL/kg, orally) for 21 days. Group II was the disease control and received rotenone (3 mg/kg, orally) for 21 days. Groups III–V received the chrysin–daidzein combination intranasally at 2.25, 1.5, and 1 mg/kg, respectively (CDNF1, CDNF2, and CDNF3 as designated in the study). Group VI was the standard-treatment group and received levodopa–carbidopa (100 + 25 mg/kg, orally) one hour before rotenone administration during days 7–21. Behavioural assessments were conducted on days 7, 14, and 21. On day 22, the animals were sacrificed for neurochemical, inflammatory, biochemical, and histopathological analyses.

2.4 Experimental design

Rotenone was prepared in sunflower oil and administered orally at 3 mg/kg each day for 21 days. Open-field activity, performance on the rotating-beam apparatus, and the stepping test were assessed on days 7, 14, and 21. On day 22, the animals were sacrificed and the brains collected. The striatum was isolated for measurement of lipid peroxidation (LPO), SOD, catalase (CAT), reduced glutathione (GSH), and neurotransmitters including dopamine (DA), glutamate, and GABA. Pro-inflammatory markers IL-6, BDNF, α-synuclein, and TNF-α were measured using ELISA kits.

2.5 Acute Oral Toxicity (OECD Guideline 423)

OECD Test Guideline 423, known as the Acute Toxic Class Method, provides a stepwise procedure for assessing acute toxicity after a single oral dose. It is designed to identify potential toxic effects and estimate the median lethal dose (LD_{50}) while limiting animal use in keeping with the principles of Replacement, Reduction, and Refinement. Female Wistar rats are commonly used because their physiology is well characterized. The test substance is administered by oral gavage at specified dose levels, commonly 5, 50, 300, or 2,000 mg/kg body weight.

After administration, each animal is observed for 14 days, with particular attention during the first four hours, for signs of toxicity, illness, or mortality. Monitoring may include the skin and fur, eyes, mucous membranes, respiratory and circulatory function, autonomic and central nervous system responses, motor activity, and behaviour. If deaths occur at a dose, a lower dose may be tested; if mortality does not occur, a higher dose may be considered. The resulting information supports classification under the Globally Harmonized System for classification and labelling of chemicals. Acute toxicity findings contribute to risk assessment, dose selection, and safety evaluation of new therapeutic candidates (OECD et al., 2001).

2.6 Analytical method development

A UV–visible spectrophotometric method was developed and validated in accordance with ICH Q2 (R1) to quantify chrysin and daidzein in samples from this study. Absorbance was measured at 315 nm for chrysin and 262 nm for daidzein. Separate stock solutions (100 µg/mL) were initially prepared using ethanol and phosphate buffer at pH 7.4 in a 1:1 ratio, following Majumder KK et al. [15].

2.7 Fabrication of nanoparticles

Chrysin- and daidzein-loaded nanoparticles were prepared using a single-emulsion solvent-evaporation procedure. The aqueous and organic phases were prepared separately. Chrysin (50 mg), daidzein (50 mg), and PLGA (100 mg) were dissolved in the organic phase using ethanol and acetone. The aqueous phase contained Tween 80 (0.45%) and polyvinyl alcohol (1%) in water. The organic phase was added gradually to the aqueous phase while probe sonication was applied to form an oil-in-water emulsion. The dispersion was then processed using a high-pressure homogenizer (Shear Jet HL 60, Dyhydromatic) at 10 kpsi with varying cycle numbers to reduce particle size. Particle size and PDI were measured using a HORIBA Zetasizer (SZ-100, version 2.40). Solvent was evaporated while stirring for 12 h. The resulting suspension was membrane-filtered and centrifuged at 15,000 rpm for 1,200 s at 4 °C. Entrapment efficiency was calculated from the clarified supernatant obtained after centrifugation [4].

2.7.1 Particle size and PDI

Particle diameter and polydispersity index (PDI) are important formulation attributes because they influence dispersion uniformity and delivery performance. Smaller particles may cross biological barriers more readily than larger particles, while a PDI below 0.3 is commonly taken to indicate a relatively uniform size distribution that may support stability and controlled release. Particle size and PDI were therefore measured with a Zetasizer as part of the nanoparticle characterization.

2.7.2 Entrapment efficiency

Entrapment efficiency (EE) describes the proportion of the initial drug amount incorporated into the nanoparticle formulation. When free drug cannot be measured directly in the carrier, the free fraction can be separated from the nanoparticles and quantified. In this study, the free drug in the supernatant following cold centrifugation was measured by UV spectrophotometry at 315 nm for chrysin and 262 nm for daidzein. EE was calculated from the difference between the total drug amount and the free drug amount, expressed as a percentage of the total drug amount.

Percent entrapment efficiency was calculated by using the following formula;

$$E.E.(\%) = \frac{\text{Total amount of the drug} - \text{Amount of free drug}}{\text{Total amount of drug}} \times 100$$

2.7.3 Zeta potential

Nanoparticle stability is influenced by both particle size and zeta potential. Zeta potential indicates the electrical potential associated with the particle surface and can affect colloidal stability as well as in vivo uptake. Previous studies have suggested that absolute zeta-potential values around or above 20 mV may support greater dispersion stability. The zeta potential of the optimized formulation was measured using a Malvern Zetasizer Nano ZS 90.

2.7.4 Drug loading efficiency and percent yield

Spray-dried nanoparticles were evaluated for drug-loading efficiency and percentage yield. Drug loading was calculated using the relationship described by Tao et al. [19], while percentage yield was determined by comparing the recovered spray-

dried product mass with the initial mass of drug, polymer, and dispersing agent [20].

$$DL\ (\%) = \text{_x0001_} \times 100$$

Percent yield was calculated as the total weight of spray dried product with respect to initial weight of drug and polymer [20]. The percent yield was calculated as:

$$\%Yield = \text{_x0001_} \times 100$$

2.7.5 X-ray diffraction studies (XRD)

X-ray diffraction (XRD) was used to examine the solid-state characteristics of the unformulated drugs and the prepared nanoparticles. Samples were analysed using Cu-Kα radiation at 40 kV and 35 mA. Diffraction data were collected across a 2θ range of 1° to 50°.

2.7.6 Differential scanning Calorimetry (DSC)

Differential scanning calorimetry (DSC) was used to examine crystallinity and thermal behaviour in pure chrysin, pure daidzein, and their nanoparticle formulations. Samples weighing 2–5 mg were dried, sealed in aluminium pans, and analysed with a Mettler-Toledo DSC 823 instrument. The temperature was increased from 25 to 300 °C at 10 °C/min while purge gas flowed at 10 mL/min. An empty sealed pan served as the reference for the thermograms (Jangid et al., 2022).

2.7.8 In vitro drug release and release kinetics

In vitro release from the optimized chrysin and daidzein nanoparticles was assessed using the method described by Kesarla et al. (2016). A dialysis membrane was soaked overnight in phosphate buffer (pH 7.4), after which 1 mL of formulation was placed inside and both ends were sealed. The membrane sac was suspended in 100 mL of the same buffer and stirred at 50 rpm at 37 ± 0.5 °C. At predetermined intervals, 5 mL samples were withdrawn and analysed spectrophotometrically at 315 and 262 nm. Each withdrawn volume was replaced with an equal volume of fresh buffer, and cumulative release was calculated before the data were fitted to release-kinetic models [21].

2.7.9 Shape and surface morphology

The surface structure and shape of nanoparticles are relevant to formulation performance and tissue tolerance. The prepared particles were therefore examined by scanning electron microscopy using a ZEISS 505/506 instrument to assess their morphology.

2.8 Experimental design

After a seven-day acclimatization period, male Albino Wistar rats were maintained in six groups as described above. Each group contained six animals weighing 200–250 g, with unrestricted access to standard laboratory feed and water. The assigned treatments were continued for 21 days, following the procedure reported by G. Srivastava et al. (2022) (Figure 1).

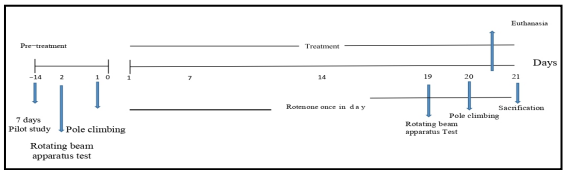


Fig 1: Schematic Representation of the Experimental Design.

2.8.1 Procedure of preclinical study:

Following acclimatization, the Albino Wistar rats were assigned to the six experimental groups, with six animals weighing 200–250 g in each group and free access to food and water. The control group received sunflower oil (1 mL/kg), while the disease group received rotenone (3 mg/kg). The standard group received rotenone together with levodopa and carbidopa (100 and 25 mg/kg, respectively). The nanoparticle groups received rotenone and intranasal CDNF at the stated low, medium, and high doses: 1, 1.5, and 2.25 mg/kg, respectively. The nanoparticle dose was selected with reference to acute toxicity testing under OECD Guideline 423.

Rotenone was administered orally for 21 consecutive days. Levodopa–carbidopa was given orally, whereas the nanoparticle formulation was administered intranasally 60 minutes before rotenone. After behavioural testing was completed, the animals were sacrificed under light anaesthesia as described in the study protocol. The brains were removed carefully and rinsed twice with chilled normal saline. Brain tissue was then isolated and homogenized in cold phosphate buffer (pH 7.4), and the supernatant was used for biochemical assays.

2.8.2 Neurobehavioral studies on experimental rats:

2.8.2.1 Open field test

The open-field test was conducted in an arena divided into 61 × 61 squares. Each rat was placed in the centre and allowed to explore for five minutes. Ambulation was assessed by counting squares crossed, and rearing was recorded when the animal rose on its hind limbs. Grooming behaviors, including face washing, licking, and scratching, were also observed, along with crossings through the central square (Calderon and Bolanos, 2011) [6]

2.8.2.2 Stepping test

The stepping test was used to assess akinesia. Each rat was supported on its forelimbs while the hind limbs were elevated, and the number of forelimb steps taken during a 30-second period was recorded (Amin et al., 2017).

2.8.2.3 Rotating beam apparatus

For the rotating-beam assessment, rats were placed facing away from a rotating rod measuring 3 cm in diameter and 90 cm in height, operating at 10 rpm. Before testing, animals were trained for three days to remain on both stationary and rotating rods, with three one-minute sessions per day. After the open-field assessment, each rat was observed for five

minutes, and the time spent on the rod was recorded (Jones and Roberts, 1968).

2.8.3 Body weight, Brain weight, and preparation of tissue homogenate

Body weight was recorded on days 1, 7, 14, and 20 to monitor changes during the induction and treatment periods. At the end of the experiment, the animals were euthanized using a high dose of isoflurane. The brains were removed, cleared of connective tissue, blotted dry, and weighed on a precision digital balance. For biochemical measurements, 10% (w/v) tissue homogenates were prepared in 0.1 M phosphate buffer (pH 7.4) and centrifuged at 13,000 rpm for 10 minutes at 4 °C. The supernatant was used to assess oxidative-stress and related biochemical parameters. Separate homogenates prepared in 0.1 M Tris-HCl buffer (pH 7.8) were used to assess steroidogenic enzyme activity. Samples were stored at an appropriate temperature until analysis (Ibrahim et al., 2022).

2.9 Biochemical Analysis

2.9.1 Proinflammatory Biomarkers (IL-6 and TNF-α)

Brain-homogenate concentrations of IL-6 and TNF-α were measured by quantitative sandwich ELISA. The assays used monoclonal antibodies specific to each cytokine and Krishgen Biosystems kits (Mumbai), following the manufacturer's instructions.

2.9.2 Oxidative stress parameters

Brain-tissue oxidative status was assessed by measuring catalase (CAT), superoxide dismutase (SOD), reduced glutathione (GSH), and malondialdehyde (MDA). Tissue was homogenized in 0.1 M phosphate buffer at pH 7.4, and the homogenate was used for protein estimation and the biochemical assays. Measurements followed standard procedures described in the literature.

2.9.3 Histological analysis

Brain sections were examined histologically after haematoxylin-and-eosin staining. Transverse sections of the cortex, midbrain, and cerebellum were fixed in formal-calcium and embedded in paraffin. Sections reported as 7–9 mm thick were cut, dewaxed in xylene, hydrated through descending alcohol concentrations, and stained with haematoxylin. They were then dehydrated through increasing alcohol concentrations, stained with 1% alcoholic eosin, differentiated in 90% alcohol, cleared in xylene, and mounted in DPX. The slides were examined using a Nikon H600L microscope.

2.9.4 Statistical analysis

Results are expressed as mean ± standard deviation (SD). Differences among groups were analysed by one-way ANOVA followed by Dunnett's multiple-comparison test. GraphPad Prism version 7.0 was used for the statistical analyses.

3 Result and discussion:

3.1 Development of Daidzein and Chrysin Nanoparticles

Formulation F8, containing 500 mg total drug, was prepared by solvent evaporation with DMSO as the organic solvent and water as the aqueous phase. The drug solution in 20 mL DMSO was added dropwise to 1,000 mL of aqueous phase containing Tween 80 (4.5 mL) and PLGA (1,000 mg), with continuous stirring. The mixture was probe-sonicated at 15,000 rpm for five minutes to produce an oil-in-water emulsion and then stirred for two hours to evaporate the solvent. Nanoparticles were collected by centrifugation at 15,000 rpm for 30 minutes at 4 °C, washed, and lyophilized with 2% mannitol as a cryoprotectant.

3.2 Experimental Design

The prepared chrysin and daidzein nanoparticles were characterized, and particle-size and entrapment-efficiency data are presented in Table 1. Across the formulations, particle size ranged from 170 to 196.1 nm and entrapment efficiency from 93% to 94%. ANOVA indicated that the formulation variables—drug-to-polymer ratio (X_1) and surfactant concentration (X_2)—significantly affected particle size and entrapment efficiency ($p < 0.05$). A higher polymer ratio tended to improve entrapment but also produced larger particles. Increasing surfactant concentration reduced particle size by stabilizing emulsion droplets, although the improvement in entrapment efficiency appeared to level off at higher concentrations. The independent variables were examined at low (−1), intermediate (0), and high (+1) coded levels. The reported values were 170 nm and 93% for daidzein nanoparticles and 196.1 nm and 94% for chrysin nanoparticles.

3.3 Statistical Analysis

A 3^2 factorial design was used to optimize PLGA nanoparticles loaded with chrysin and daidzein. The effects of PLGA concentration (X_1) and high-pressure homogenization (HPH) cycle number (X_2) were examined against three responses: particle size (Y_1), polydispersity index (Y_2), and entrapment efficiency (Y_3). HPH pressure was held constant at 10 kpsi throughout the experiments.

Chrysin						
1	F1	50	12	192	0.24	79
2	F2	50	10	202	0.29	75
3	F3	50	8	222	0.3	71
4	F4	100	10	212	0.29	85
5	**F5**	**100**	**12**	**196.1**	**0.27**	**88**
6	F6	100	8	245	0.32	82
7	F7	150	10	312	0.39	92
8	F8	150	8	359	0.41	90
9	F9	150	12	296	0.34	95

Table no.1: Optimization of nanoparticles with coded levels and translation in actual units along with responses.

Respones	Model	R^2	Adjusted R^2	PredictedR^2	SS	DF	MS	F value	P value	Model significance
Y1	Quadratic	0.9986	0.9963	0.9832	4444.10	2	2222.05	166.84	0.0008	Significant
Y2	Quadratic	0.9874	0.9663	0.8898	0.0026	2	0.0013	12.89	0.0336	Significant
Y3	Quadratic	0.9996	0.9990	0.9957	3.61	2	1.81	27.86	0.0115	Significant

Table no.2: Summary of results of regression analysis and ANOVA for measured responses.
SS: Sum of Square; DF: Degree of freedom; MS: mean square

Model fitting indicated that quadratic equations best described particle size (R_1) and PDI (R_2), whereas a linear model was selected for entrapment efficiency (R_3). The reported p-value was below 0.05, supporting statistical significance of the model (Table 2). The fitted equations are presented below.

The following equations were suggested for the responses;

_x0001_^{2}+9.68X2^2

_x0001_X2^2

Runs	fc	A-PLGA Conc.mg	B-HPH Cycles	Particle size nm	PDI	%EE
1	F1	50	12	240	0.37	72.89
2	F2	50	10	192	0.30	89.90
3	F3	50	8	202	0.31	87.00
4	F4	100	10	232	0.36	75.95
5	**F5**	**100**	**12**	**170.4**	**0.34**	**93**

Response	Model	R^2	Adjusted R^2	PredictedR^2	SS	DF	MS	F value	P value	Model significance
Y1	Quadratic	0.9869	0.9650	0.8614	8941.24	2	4470.62	34.63	0.0085	Significant
Y2	Linear	0.9944	0.9926	0.9867	0.0367	2	0.0184	536.35	< 0.0001	Significant
Y3	Linear	0.9928	0.9904	0.9806	742.17	2	371.08	413.16	<0.0001	Significant

$$Y3 = 84.89 + 8.67X1 + 3.17X2 - 0.7500 - 1.332 + 0.1667$$

The equations indicate that increasing HPH cycle-related processing reduced particle size and PDI while improving entrapment efficiency. In contrast, increasing PLGA concentration raised all three responses. The effect attributed to PLGA concentration was approximately twice as strong as that associated with HPH processing. The three-dimensional response-surface plots in Figure 2 illustrate how the two independent variables relate to the measured outcomes.

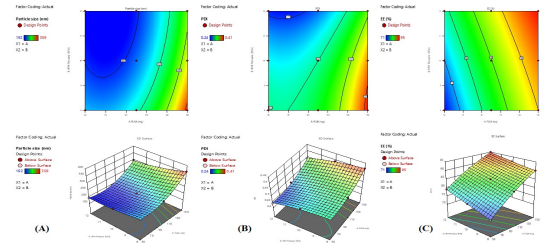


Fig 2: 2D, 3D counter plot of Chrysin (A) Particle Size, (B) Polydispersity index, (C) Entrapment Efficiency.

Daidzein						
6	F6	100	8	196	0.30	89.90
7	F7	150	10	256	0.40	67.43
8	F8	150	8	205	0.32	84.28
9	F9	150	12	215	0.33	81.73

Table no.3: Optimization of nanoparticles with coded levels and translation in actual units along with responses.

Table no.4: Summary of results of regression analysis and ANOVA for measured responses.
SS: Sum of Square; DF: Degree of freedom; MS: mean square

For daidzein nanoparticles, the software likewise selected quadratic models for particle size (R_1) and PDI (R_2), and a linear model for entrapment efficiency (R_3). The p-value was below 0.05, indicating that the model was statistically significant (Table 4). The corresponding fitted equations are provided below.

The following equations were suggested for the responses;

$$_x0001_^{2}+15.53X2^{2}$$

$$Y2 = 0.3422 + 0700 - 0.0350$$

$$Y3 = 79.22 + 10.50X1 + 3.67X2$$

The model results for daidzein showed the same overall pattern: increased HPH cycling was associated with smaller particles and lower PDI, alongside higher entrapment efficiency (Table 4). Greater PLGA concentration increased the responses, and its estimated influence was roughly twice that of HPH processing. Figure 3 presents the response-surface plots for the interaction of the independent variables and the selected outcomes.

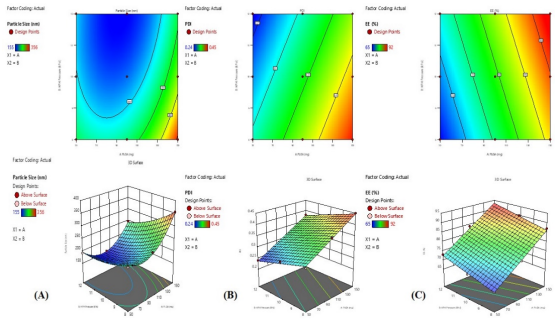


Fig3: 2D, 3D counter plot of Daidzein (A) Polydispersity index, (B) Particle Size, (C) Entrapment Efficiency.

3.4 Nanoparticle Characterization:

3.4.1 FTIR Analysis

FTIR spectroscopy was used to examine possible interactions between the drug compounds and formulation components. Figure 4 compares spectra from pure daidzein, pure chrysin, daidzein nanoparticles, and chrysin nanoparticles. Differences in the positions and intensities of characteristic absorption bands suggest changes in the compounds' vibrational environments after formulation and are consistent with drug–excipient interactions, including possible hydrogen bonding.

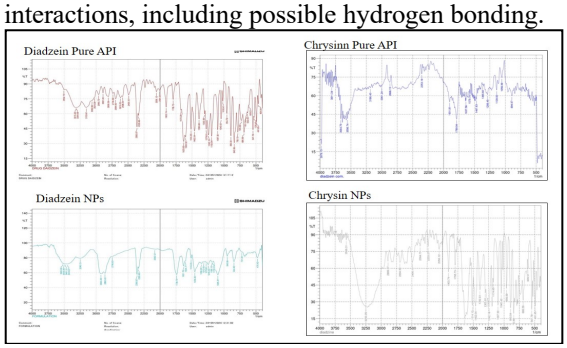


Fig 4: Fourier Transform Infrared (FTIR) Spectra. This figure presents the FTIR spectra for pure Daidzein, pure Chrysin, Daidzein NP, and Chrysin NP, illustrating changes in characteristic absorption bands due to formulation.

3.4.2 DSC and XRD Analysis:

DSC and XRD were used to assess the thermal and crystalline properties of the chrysin and daidzein formulations. The DSC thermograms in Figures 5A and 5B showed thermal events in the formulated samples that differed from those of the raw compounds, indicating a change in solid-state behaviour. The XRD patterns in Figures 5C and 5D also differed from those of the starting materials, providing further evidence of changes in the crystalline characteristics of the formulations.

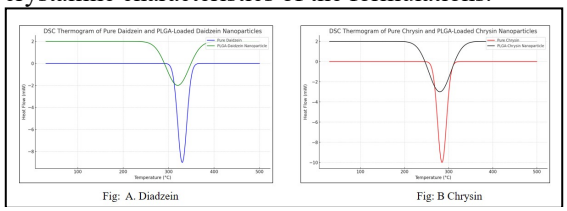


Fig5A: DSC thermogram of the Formulation of (A) Daidzein, (B) Chrysin.

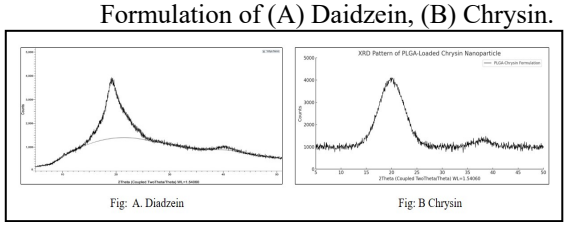


Fig5B: XRD of Formulation of (A) Daidzein, (B) Chrysin.

3.4.3 Particle Size, Zeta Potential, and PDI:

Particle size, zeta potential, and PDI were measured to characterize the formulations. The daidzein preparation showed a Z-average particle size as reported in the associated figure, while the chrysin preparation was assessed using the same measurements. These parameters were used together to evaluate particle-size distribution and the likely physical stability of the nanoparticle dispersions.

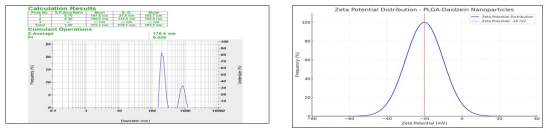


Fig6A: Particle size Distribution and Zeta Potential of Daidzein

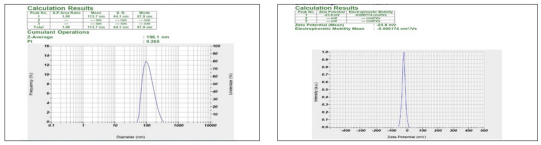


Fig6B: Particle size Distribution and Zeta Potential of Chrysin

3.4.4 Morphological Analysis (FE-SEM):

The morphology of the prepared formulations was examined by scanning electron microscopy. As shown in Figure 7, the daidzein nanoparticles appeared relatively uniform in shape and had a comparatively smooth surface. The micrographs were used to assess particle shape and surface characteristics following formulation.

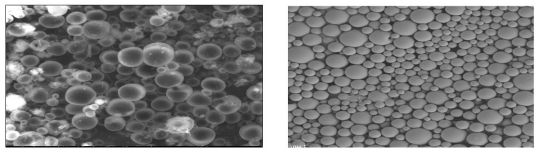


Fig7: Scanning Electron Microscopy (SEM) Images of Nanoparticles (A) Daidzein nanoparticles, (B) Chrysin nanoparticles.

3.4.5 Neurobehavioral studies on experimental rats:

During the five-minute open-field test in a 61 × 61 cm arena, the normal-control and medium-dose treatment groups displayed more typical locomotor activity than the rotenone-treated disease-control group, which showed reduced movement.

3.4.5.1 Open field test

Pretreatment with CDNF1, CDNF2, and CDNF3 at 2.25, 1.5, and 1 mg/kg, respectively, significantly reduced immobility compared with the disease-control group (***P < 0.0001). Rearing frequency and the activity index were also assessed as indicators of the behavioural effects of rotenone and treatment.

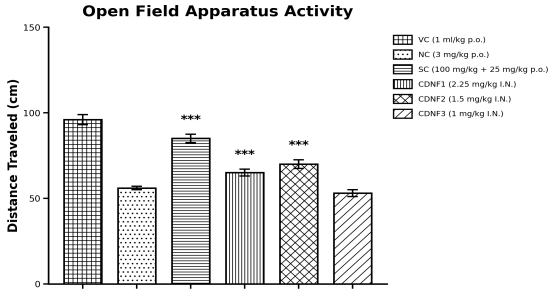


Fig 8: Neurobehavioral studies of open field apparatus activity.

Data expressed as mean ±SEM. N=6: ***P<0.0001 compared with negative control, ###P<0.0001 when compared with normal control using one-way ANOVA followed by Dunnett's test as post ANOVA test using GraphPad prism 9.4 software.

3.4.5.2 Stepping test

The CDNF1–3 groups (2.25, 1.5, and 1 mg/kg) showed a significant increase in adjusting steps relative to the disease-control group (***P < 0.0001), particularly in the forelimb direction. This change is consistent with improved performance on the stepping task.

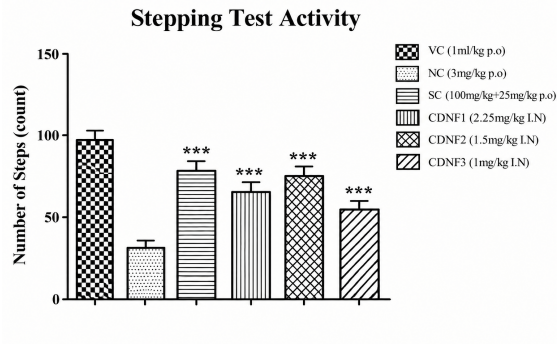


Fig 9: Neurobehavioral studies of Stepping Test activity.

Data Expressed are mean ± SEM (n = 6). ***P < 0.0001 vs. negative control, ###P < 0.0001 vs. normal control one-way ANOVA with Dunnett's test, GraphPad Prism 9.4.

3.4.5.3 Rotating beam apparatus:

In the rotating-beam assessment, the principal outcome was the time each animal remained on the rod before falling. Animals treated with CDNF1–3 at 2.25, 1.5, and 1 mg/kg showed a significant improvement compared with the disease-control group (***P < 0.0001), as presented in Figure 10.

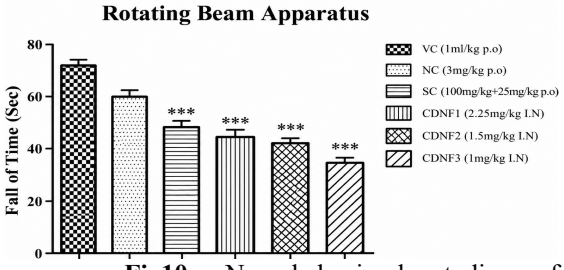


Fig10: Neurobehavioral studies of Rotating beam apparatus activity

Data expressed as mean ±SEM. N=6: ***P<0.0001 compared with negative control, ###P<0.0001 when compared with normal control using one-way ANOVA followed by Dunnett's test as post ANOVA test using GraphPad prism 9.4 software.

3.4.5 Preclinical Study of Parkinson Disease:

3.4.5.1 Inflammatory Biomarkers

Compared with normal controls, rotenone-treated animals showed higher levels of the inflammatory markers TNF-α and IL-6. Treatment with chrysin–daidzein nanoparticles reduced these markers, with the response varying by dose. The medium-dose formulation produced a particularly clear reduction, bringing the measured values closer to those in the normal and standard-treatment groups. These results support a potential anti-inflammatory effect in this model (Figures 11 and 12).

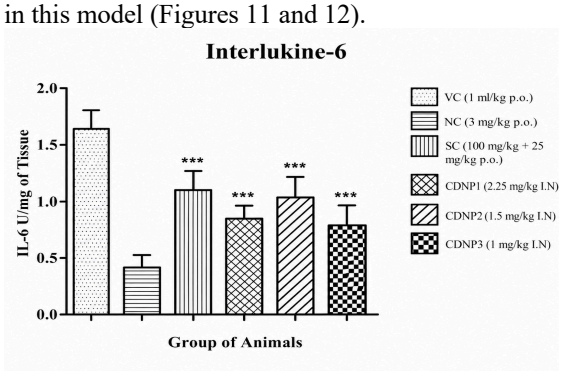


Fig11: Effect of Daidzein and Chrysin nanoparticle therapy on (A) Interleukin – 6 Levels.

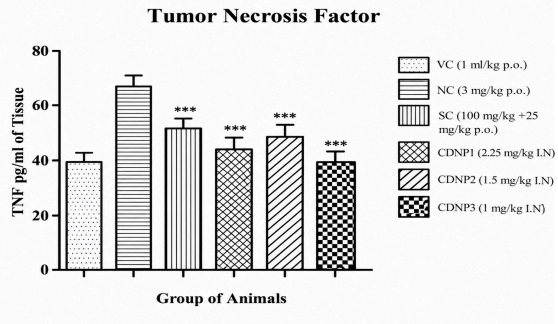


Fig12: Effect of Daidzein & Chrysin nanoparticle therapy on(B) TNF α Levels.

Data is expressed as a Mean ± SEM, n = 6. One-way ANOVA were used for statistical analysis, followed by Dunnet multiple comparison test. ***p<0.001 vs Let group; ###p<0.001 vs Control group.

3.4.5.2 Oxidative Stress Markers

Rats exposed to rotenone showed evidence of increased oxidative stress, including higher MDA levels and lower SOD, CAT, and GSH activity than normal controls (Figures 13–16). Administration of chrysin–daidzein nanoparticles improved these measures in a dose-related pattern. The medium-dose group showed reduced MDA and increased SOD, CAT, and GSH values, approaching those observed in the normal and standard-treatment groups. The findings are consistent with an antioxidant effect of the nanoparticle treatment in this experimental model.

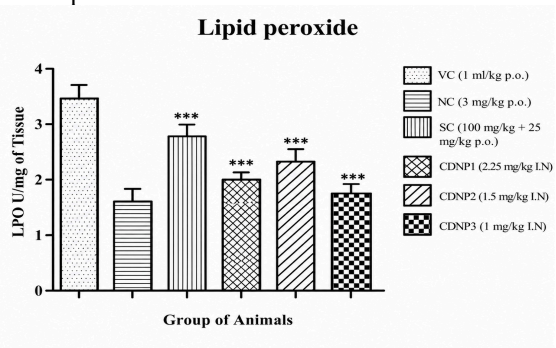
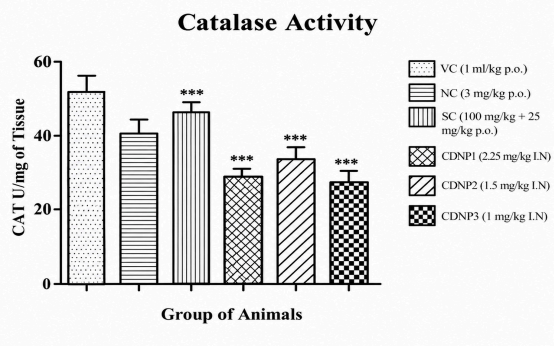


Fig13: Effect of Daidzein and Chrysin nanoparticle therapy on (A) LPO Levels.



- **Fig14:** Effect of Daidzein and Chrysin nanoparticle therapy on (B) CAT Levels.

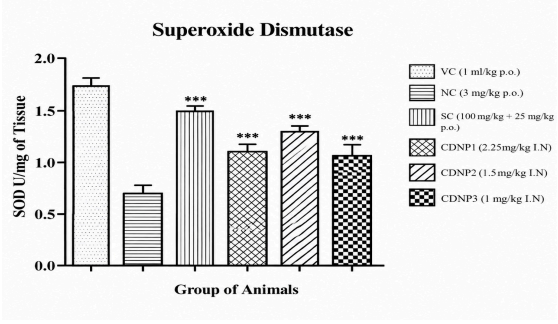


Fig15: Effect of Daidzein and Chrysin nanoparticle therapy on (C) SOD Levels.

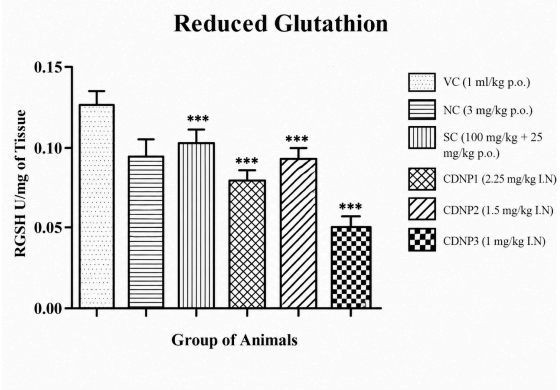


Fig 16: Effect of Daidzein and Chrysin nanoparticle therapy on Reduced Glutathione Level (D) (RGSH) Levels.

Data is expressed as a Mean ± SEM, n = 6. One-way ANOVA were used for statistical analysis, followed by the Dunnett's multiple comparison test. ***p<0.001 vs Let group; ###p<0.001 vs Control group.

3.4.5.3 Histopathology of Brain Tissue

Examination of the nasal mucosa did not reveal irritation attributable to the formulation, supporting its local tolerability under the conditions tested. In the rotenone-induced rat model, combined chrysin and daidzein treatment was associated with higher dopamine levels than the monotherapy comparison groups. SOD, GSH, and catalase values also improved, in keeping with the biochemical findings described above.

Histological assessment showed marked differences between brain tissue from rotenone-treated animals and normal controls (Figure 17). The disease-control group displayed neuronal degeneration and nuclear pyknosis. These changes were less pronounced in animals treated with chrysin–daidzein nanoparticles. Improvement was most evident in the medium-dose group, whose tissue appearance more closely resembled that of the normal controls; the low-dose group also showed some improvement.

The plain-compound group showed less histological improvement than the nanoparticle-treated groups. The standard-treatment group receiving levodopa and carbidopa also showed substantial recovery, with findings comparable to those observed in the medium-dose nanoparticle

group.

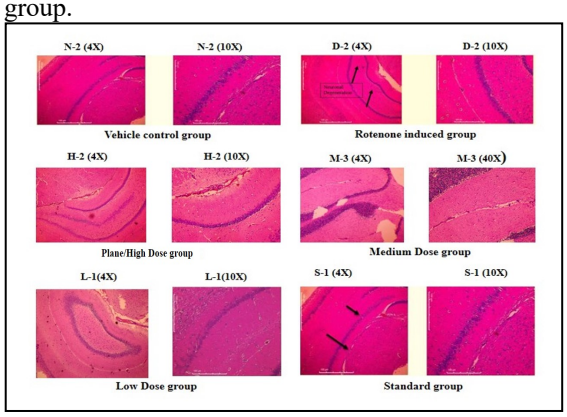


Fig 17: Histopathological Examination of Brain.
This figure displays significant Histopathological photomicrographs of Brain sections from different experimental groups.

3 Discussion:

This study examined whether PLGA-based nanoparticles containing chrysin and daidzein could protect against rotenone-induced Parkinsonian changes in Albino Wistar rats. Rotenone was used because it can reproduce features associated with PD, including oxidative stress, mitochondrial dysfunction, and dopaminergic neurodegeneration. Pilot histopathological observations informed the choice of oral rather than subcutaneous rotenone administration to limit toxicity and mortality. Nanoparticles were produced following high-pressure homogenization and spray drying. Of the nine formulations prepared using a central composite design, Batch 6 was reported to have favourable characteristics: zeta potentials of −23.8 and −20 mV, particle sizes of 196.1 nm for chrysin and 170.4 nm for daidzein, and improved in vitro release (53.12 ± 1.4% over 10 hours). FTIR and DSC results were interpreted as supporting drug–excipient compatibility and amorphization, which may contribute to improved solubility and bioavailability.

Behavioural testing showed substantial motor impairment in the rotenone group. By comparison, the medium- and high-dose nanoparticle groups displayed better coordination and less akinesia, with performance closer to that of normal controls. Biochemical measurements also indicated higher SOD, CAT, and GSH levels and lower MDA in nanoparticle-treated animals than in the rotenone group. BDNF expression, which was reduced following rotenone exposure, showed dose-related recovery and reached its highest reported level at 2.25 mg/kg.

Chrysin- and daidzein-loaded nanoparticles (CDN) were prepared and optimized using a 3^2 factorial design. PLGA concentration (X_1) and HPH cycle number (X_2) were evaluated for their effects on particle size (Y_1), PDI (Y_2), and entrapment efficiency (Y_3), while HPH pressure remained fixed at 10 kpsi. The variables were assessed at three coded levels, and the resulting particle-size values were reported in the formulation tables. Statistical analysis indicated model significance at $p < 0.05$.

PLGA concentration showed a positive association with all measured responses. As polymer concentration increased, particle size and PDI also increased, potentially because greater viscosity reduced the efficiency of shear forces during homogenization. Higher polymer levels may also provide more matrix material for drug entrapment. Similar observations have been reported by Kakad et al. (2021) [11]. In contrast, increasing the number of HPH cycles was associated with greater entrapment efficiency and reductions in particle size and PDI.

The decrease in particle size and PDI with additional homogenization cycles is consistent with greater shear acting on the dispersed material; these conditions may also improve drug loading in polymeric carriers [10,12]. Response-surface plots further illustrate the relationships between formulation variables and outcomes. Overall, the study developed a PLGA-based formulation for intranasal delivery in a PD model. The reported nanoparticles had a zeta potential of −24.86 ± 2.286 mV, a PDI of 0.107 ± 0.0316, a spherical and relatively uniform morphology, and an average particle size of 365.03 ± 6.8 nm. Release experiments reported 90.52% in vitro and 68.67% ex vivo drug release at 24 hours.

Taken together, the findings suggest that chrysin- and daidzein-loaded PLGA nanoparticles may lessen rotenone-associated neurotoxicity in this model. The observed changes included improved antioxidant measures, recovery of BDNF levels, and better behavioural and motor outcomes.

4 Conclusion:

Overall, intranasal delivery of chrysin- and daidzein-loaded PLGA nanoparticles was associated with improved antioxidant status, greater brain availability, and reduced neurodegenerative symptoms in the rotenone-induced rat model. This non-invasive nose-to-brain approach merits further investigation as a potential strategy for treating Parkinson's disease. The present preclinical findings do not, however, establish clinical efficacy in humans.

5 References

1. Pringsheim T, et al. "The prevalence of Parkinson's disease: A systematic review and meta-analysis." *Movement Disorders.* 2014 Nov; 29(13):1583-90. https://doi.org/10.1002/mds.25945
2. Dashputre, N. L., Laddha, U. D., Patil, S. B., Kadam, J. D., & Kshirsagar, S. J. (2023). An insight to development and in-vitro, ex-vivo, in-vivo study of naringenin

nanoparticles against letrozole induced polycystic ovarian syndrome in female wistar rats. *Journal of Drug Delivery Science and Technology*, *90*, 105129. https://doi.org/10.1016/j.jddst.2023.105129

3. Verma, R. and Nehru, B., 2009. Effect of centrophenoxine against rotenone-induced oxidative stress in an animal model of Parkinson's disease. *Neurochemistry international*, *55*(6), pp.369-375.
4. Laddha, U.D., Dashputre, N. L., Chikhale, S.S.,., Gaikwad, S.S., Moravkar, K.K. and Kshirsagar, S.J., 2023. Development and in vitro, ex vivo, in vivo investigation of curcumin loaded nanoparticles in management of dry eye disease. *Journal of Drug Delivery Science and Technology*, *87*, p.104802.
5. Peshattiwar, V., Muke, S., Kaikini, A., Bagle, S., Dighe, V. and Sathaye, S., 2021. Evaluation of Daidzein Against Rotenone Induced Parkinson's Disease and a Potential Involvement of Mitochondrial Biogenesis.
6. Von Wrangel, C., Schwabe, K., John, N., Krauss, J.K. and Alam, M., 2015. The rotenone-induced rat model of Parkinson's disease: behavioral and electrophysiological findings. *Behavioural brain research*, *279*, pp.52-61.
7. Kalia LV, Lang AE. "Parkinson's disease." *The Lancet.* 2015 Aug 29;386(9996):896-912. https://doi.org/10.1016/S0140-6736(14)61393-3
8. Poewe W, et al. "Parkinson disease." *Nature Reviews Disease Primers.* 2017 Mar 23;3(1):17013. https://doi.org/10.1038/nrdp.2017.13
9. Sharma, N., Khurana, N., Muthuraman, A. and Utreja, P., 2021. Pharmacological evaluation of vanillic acid in rotenone-induced Parkinson's disease rat model. *European journal of pharmacology*, *903*, p.174112.
10. Cannon, J.R., Tapias, V., Na, H.M., Honick, A.S., Drolet, R.E. and Greenamyre, J.T., 2009. A highly reproducible rotenone model of Parkinson's disease. *Neurobiology of disease*, *34*(2), pp.279-290.
11. Shankar, J., Geetha, K.M. and Wilson, B., 2021. Potential applications of nanomedicine for treating Parkinson's disease. *Journal of Drug Delivery Science and Technology*, *66*, p.102793.
12. Alberto Ascherio, Michael A Schwarzschild, The epidemiology of Parkinson's disease risk factors and prevention, The Lancet Neurology, Volume 15, Issue 12, 2016, Pages1257-1272
13. Patel T, Zhou J, Piepmeier JM, Saltzman WM. "Polymeric nanoparticles for drug delivery to the central nervous system." *Adv Drug Deliv Rev.* 2012; 64 (7): 701-705. https://doi.org/10.1016/j.addr.2011.11.002
14. Saraiva C, et al. "Nanoparticle-mediated brain drug delivery: Overcoming blood-brain barrier to treat neurodegenerative diseases." *Journal of Controlled Release.* 2016 May 10; 235: 34-47. https://doi.org/10.1016/j.jconrel.2016.05.044
15. Langston JW, Langston EB, Irwin I, MPTP-induced Parkinsonism in human and non-human primates—clinical and experimental aspects, Acta Neurologica Scandinavica, Supplementum, 1984, 100:49-54.
16. Trzaska KA, Rameshwar P. (2007) Current advances in the treatment of Parkinson's disease with stem cells, Curr Neurovasc Res. 4: 99-109.
17. Broggi G, Franzini A, Tringali G, Ferroli P, Marras C, Romito L, Maccagnano E. (2006) Deepbrain stimulation as a functional scalpel. Acta Neurochir Suppl. 99:13-19.
18. Garima Srivastava, Anubhuti Dixit, Sharawan Yadav, Devendra Kumar Patel,OmPrakash, Mahendra Pratap Singh (2012), "Resveratrol potentiates cytochrome P450 2d22-mediated neuroprotection in maneb-andparaquat-induced parkinsonism in the mouse", Free Radical Biology & Medicine, Elsevier,1294-1306.
19. Jangid, A.K., Solanki, R., Patel, S., Medicherla, K., Pooja, D. and Kulhari, H., 2022. Improving anticancer activity of chrysin using tumor microenvironment pH-responsive and self-assembled nanoparticles. *ACS omega*, *7*(18), pp.15919-15928.
20. Suman Patel, Virendra Singh, Abhai Kumar, Yogendra Kumar Gupta, Mahendra Pratap Singh (2006),"Status of antioxidant defense system and expression of toxic antresponsive genesin striatum of maneb-andparaquat-induced Parkinson's disease phenotype in mouse: Mechanism of neurodegeneration", Brain

research, Elsevier,9-18.
21. Jay Prakash, Satyndra Kumar Yadav, Shikha Chouhan, Surya Pratap Singh (2013), "Neuroprotective Role of Withania somnifera Root Extract in Maneb–Paraquat Induced Mouse Model of Parkinsonism", Neurochem, Springer, 38:972-980.

Funding Details: This study was financially supported by ASPIRE-Research Mentorship Grant from Savitribai Phule Pune University, Pune (IQAC/540/2026).

Conflict of interest

The authors declare no conflict of interest.

Data availability statement

The data that support the findings of this study are available from the corresponding author upon reasonable request.

Acknowledgements

The authors are thankful to the Department of Science and Technology (DST), Govt. of India for the FIST grant (SR/FST/COLLEGE-2024/1648) that supported the establishment of the Particle Size Analyzer facility.